

Orbitally forced ice sheet fluctuations during the Marinoan Snowball Earth glaciation

Benn, Douglas I.; Le Hir, Guillaume; Bao, Huiming; Donnadieu, Yannick; Dumas, Christophe; Fleming, Edward J.; Hambrey, Michael J.; McMillan, Emily A.; Petronis, Michael S.; Ramstein, Gilles; Stevenson, Carl T. E.; Wynn, Peter M.; Fairchild, Ian J.

DOI:
[10.1038/ngeo2502](https://doi.org/10.1038/ngeo2502)

License:
None: All rights reserved

Document Version
Peer reviewed version

Citation for published version (Harvard):
Benn, DI, Le Hir, G, Bao, H, Donnadieu, Y, Dumas, C, Fleming, EJ, Hambrey, MJ, McMillan, EA, Petronis, MS, Ramstein, G, Stevenson, CTE, Wynn, PM & Fairchild, IJ 2015, 'Orbitally forced ice sheet fluctuations during the Marinoan Snowball Earth glaciation', *Nature Geoscience*, vol. 8, no. 9, pp. 704-707.
<https://doi.org/10.1038/ngeo2502>

[Link to publication on Research at Birmingham portal](#)

Publisher Rights Statement:

Final Version of Record published as: Benn, Douglas I., et al. "Orbitally forced ice sheet fluctuations during the Marinoan Snowball Earth glaciation." *Nature Geoscience* 8.9 (2015): 704-707. Available online: <http://dx.doi.org/10.1038/ngeo2502>

Checked October 2015

General rights

Unless a licence is specified above, all rights (including copyright and moral rights) in this document are retained by the authors and/or the copyright holders. The express permission of the copyright holder must be obtained for any use of this material other than for purposes permitted by law.

- Users may freely distribute the URL that is used to identify this publication.
- Users may download and/or print one copy of the publication from the University of Birmingham research portal for the purpose of private study or non-commercial research.
- User may use extracts from the document in line with the concept of 'fair dealing' under the Copyright, Designs and Patents Act 1988 (?)
- Users may not further distribute the material nor use it for the purposes of commercial gain.

Where a licence is displayed above, please note the terms and conditions of the licence govern your use of this document.

When citing, please reference the published version.

Take down policy

While the University of Birmingham exercises care and attention in making items available there are rare occasions when an item has been uploaded in error or has been deemed to be commercially or otherwise sensitive.

If you believe that this is the case for this document, please contact UBIRA@lists.bham.ac.uk providing details and we will remove access to the work immediately and investigate.

Orbitally Forced Ice Sheet Fluctuations in Snowball Earth

Douglas I. Benn,^{1,2*} Guillaume Le Hir,³ Huiming Bao,⁴ Yannick Donnadieu,⁵ Christophe Dumas,⁵ Edward J. Fleming,^{1,6,7} Michael J. Hambrey,⁸ Emily A. McMillan,⁶ Michael S. Petronis,⁹ Gilles Ramstein,⁵ Carl T.E. Stevenson,⁶ Peter M. Wynn,¹⁰ Ian J. Fairchild⁶

¹Department of Geology, The University Centre in Svalbard (UNIS), N-9171 Longyearbyen, Norway.

²School of Geography and Geosciences, University of St Andrews, St Andrews KY16 8YA, Scotland, UK.

³Institut de Physique du Globe de Paris, Paris, France

⁴Department of Geology and Geophysics, E235 Howe-Russell Complex, Louisiana State University, Baton Rouge, LA 70803, USA.

⁵Laboratoire des Sciences du Climat et de l'Environnement, CNRS-CEA, Gif-sur-Yvette, France

⁶School of Geography, Earth and Environmental Sciences, University of Birmingham B15 2TT, UK.

⁷Current address: CASP, West Building, 181A Huntingdon Road, Cambridge, CB3 0DH, UK

⁸Institute of Geography and Earth Sciences, Aberystwyth University, Aberystwyth, Wales, UK.

⁹Natural Resource Management, Environmental Geology,, New Mexico Highlands University, Las Vegas, New Mexico, USA.

¹⁰Lancaster Environment Centre, University of Lancaster, Lancaster LA1 4YQ, UK.

*Corresponding author. E-mail: Doug.Benn@unis.no

1 Snowball Earth theory provides a powerful framework for understanding
2 Neoproterozoic panglaciations, although some of its predictions are apparently
3 contradicted by geological evidence. For example, Snowball theory posits that the
4 panglaciations were terminated after millions of years of fridity by a positive
5 feedback, in which initial warming from rising atmospheric CO₂ was amplified by
6 reduction of ice cover and planetary albedo (1, 2). This threshold behaviour implies
7 that most of the glacial record was deposited in a brief 'melt-back' period (3), an
8 interpretation apparently inconsistent with geological evidence for glacial-
9 interglacial cycles in low palaeolatitudes (4-6). Here we use geological and
10 geochemical evidence combined with numerical modeling experiments to
11 reconcile these apparently conflicting views. New evidence from Svalbard
12 (Norwegian High Arctic) indicates oscillating glacier extent and hydrological
13 conditions within continental deposits of a Cryogenian glaciation, during a period
14 when pCO₂ was uniformly high. Modeling experiments show that such oscillations
15 can be explained by orbital forcing in the late stages of a 'Snowball' glaciation,
16 while pCO₂ was rising towards the threshold required for complete melt-back. This
17 reconciles Snowball Earth theory with evidence for the complex successions
18 observed at many other localities.

19 The Wilsonbreen Formation in NE Svalbard contains a detailed record of
20 environmental change during the Marinoan, the second of the major Cryogenian
21 glaciations (650-635 Ma) (7, 8). At this time, Svalbard was located in the Tropics on
22 the eastern side of Rodinia (9, 10). The Wilsonbreen Formation is up to up to 180 m
23 thick and was deposited within a long-lived intracratonic sedimentary basin (11). It is
24 subdivided into three members (W1, W2 and W3) based on the relative abundance

25 of diamictite and carbonate beds (7, 8; Fig. 1; Supplementary Figures 1 & 2). The
26 occurrence of lacustrine sediments containing both precipitated carbonate and
27 ice-rafted detritus throughout the succession, and intermittent evaporative
28 carbonates and fluvial deposits, indicates ~~deposition in a closed terrestrial basin.~~
29 ~~That~~ the basin remained isolated from the sea throughout deposition of the
30 Wilsonbreen Formation, ~~consistent with due to~~ eustatic sea level fall of several
31 hundred metres ~~during the Marinoan and limited local isostatic depression~~
32 (Supplementary Information; 12). This makes it an ideal location to investigate the
33 possibility of climate cycles within a Neoproterozoic panglaciation, as it provides
34 direct evidence of subaerial environments and climatic conditions.

35 We made detailed sedimentary logs at ten known and new localities extending
36 over 60 km of strike (Fig. 1; Supplementary Figure 1; see Methods). Seven sediment
37 facies associations were identified, recording distinct depositional environments that
38 varied in spatial extent through time (Supplementary Figure 3; Supplementary
39 Information). These are: FA1: *Subglacial*, recording direct presence of glacier ice,
40 FA2: *Fluvial channels*, FA3: *Dolomitic floodplain*, recording episodic flooding,
41 evaporation and microbial communities; FA4: *Carbonate lake margin*, including
42 evidence of wave action; FA5: *Carbonate lacustrine*, including annual rhythmites and
43 intermittent ice-rafted debris; FA6: *Glacilacustrine*, consisting of ice-proximal
44 grounding-line fans (FA6-G) and ice-distal rainout deposits (FA6-D); and FA7:
45 *Periglacial*, recording cold, non-glacial conditions. Additional descriptions are
46 provided in the Supplementary Information. The vertical and horizontal distribution
47 of these facies associations (Fig. 1) allows the sequence of environmental changes to
48 be reconstructed in detail.

49 (1) The base of the Formation is a well-marked periglacially weathered horizon
50 with thin wind-blown sands (Supplementary Figure 4a-b). This surface records very
51 limited sediment cycling in cold, arid conditions.

52 (2) At all localities, the weathering horizon is overlain by fluvial channel facies
53 (FA2) and mudstones, marking the appearance of flowing water in the basin and
54 implying positive air temperatures for at least part of the time (Supplementary
55 Figure 5a).

56 (3) Glacilacustrine deposits (FA6-D) record flooding of the basin and delivery of
57 sediment by ice-rafting (Supplementary Figure 4c-d). Far-travelled clasts are
58 common, indicating transport by a large, continental ice sheet.

59 (4) Warm-based, active ice advanced into the basin, indicated by traction tills and
60 glacitectonic shearing (FA1; Supplementary Figure 4e-g).

61 (5) Ice retreat is recorded by a second periglacial weathering surface (FA7)
62 developed on unconsolidated sediment at the top of member W1. This is overlain by
63 fluvial channel, floodplain, lake-margin and carbonate lacustrine sediments of W2
64 (FA2-5; Supplementary Figure 5), recording a shifting mosaic of playa lakes and
65 ephemeral streams. Lakes and river channels supported microbial communities.
66 Millimetre-scale carbonate-siliciclastic rhythmites indicate seasonal cycles of
67 photosynthesis. Overall, the environment appears to have been closely similar to
68 that of the present-day McMurdo Dry Valleys in Antarctica, though with less extreme
69 seasonality due to its low latitude (13).

70 (6) Water levels and glacier extent underwent a series of oscillations, recorded by
71 switches between glacilacustrine diamictite (FA6-D) and fluvial, lacustrine and lake-
72 margin sediments (FA2-5) in member W2. Sedimentation rates inferred from annual

73 rhythmites in member W2 suggest that each retreat phase may have lasted $\sim 10^4$
74 years.

75 (7) A second major ice advance marks the base of W3, with widespread
76 deposition of subglacial tills and glacitectonism of underlying sediments. Basal tills
77 are absent from the northernmost locality, but close proximity of glacier ice is
78 recorded by grounding-line fans (FA6-G; Supplementary Figure 4h-i).

79 (8) Ice retreated while the basin remained flooded and glacial sediment
80 continued to be delivered to the lake by ice rafting. Thin laminated carbonates (FA5)
81 in W3 indicate periods of reduced glacial sedimentation, indicative of minor
82 climatic fluctuations over timescales of $\sim 10^3$ years (Supplementary Figure 5g).

83 (9) A sharp contact with overlying laminated 'cap' carbonate (Supplementary
84 Figure 2) records the transition to post-glacial conditions. At some localities, basal
85 conglomerates provide evidence of subaerial exposure followed by marine
86 transgression. The cap carbonate closely resembles basal Ediacaran carbonates
87 elsewhere, and marks global deglaciation, eustatic sea-level rise and connection of
88 the basin to the sea (1, 12, 14).

89 Environmental and atmospheric conditions during deposition of W2 and W3 can
90 be further elucidated by isotopic data from carbonate-associated sulphate in
91 lacustrine limestones (Fig. 2 and Supplementary Figure 6). These display negative to
92 extremely negative $\Delta^{17}\text{O}$ values with consistent linear co-variation with $\delta^{34}\text{S}$,
93 indicating mixing of pre-glacial sulphate and isotopically light sulphate formed in a
94 CO_2 -enriched atmosphere (15, 16). The observed values could reflect non-unique
95 combinations of $p\text{CO}_2$, $p\text{O}_2$, O_2 residence time and other factors, but a box model
96 (17) indicates $p\text{CO}_2$ was most likely ~ 10 to 100 mbar (1 mbar = 1000 ppmv).

97 These values are too high to allow formation of low-latitude ice sheets in the
98 Neoproterozoic, but they are consistent with a late-stage Snowball Earth. For an ice-
99 free Neoproterozoic Earth, model studies indicate mean terrestrial temperatures in
100 the range 30-50°C for $p\text{CO}_2 = 10$ to 100 mbar (18). Formation of low-latitude ice
101 sheets requires much lower $p\text{CO}_2$, on the order of 0.1 - 1 mbar (2, 19, 20), but once
102 formed, high albedo ice cover can maintain low planetary temperatures despite
103 rising $p\text{CO}_2$. This hysteresis in the relationship between $p\text{CO}_2$ and planetary
104 temperature is a key element of Snowball Earth theory. It implies that W2 and W3
105 were deposited relatively late in the Marinoan, after volcanic outgassing had raised
106 $p\text{CO}_2$ from 0.1 or 1 mbar to 10 or 100 mbar. Modelled silicate weathering and
107 volcanic outgassing rates indicate that this would require 10^6 to 10^7 years (21).

108 The consistent co-variation of $\Delta^{17}\text{O}$ and $\delta^{34}\text{S}$ in lacustrine limestones in both W2
109 and W3 suggests no detectable rise in atmospheric $p\text{CO}_2$, as this would alter the
110 slope of the mixing line (Fig. 2). This implies that the glacier oscillations recorded
111 in deposition of both W2 and W3 occurred in during a relatively short time interval
112 ($<10^5$ years, 21). ~~We therefore infer that the glacier oscillations recorded in the~~
113 ~~Wilsonbreen Formation occurred during a relatively brief period~~ toward the end of
114 the Marinoan. ~~whereas the much longer period during which~~ This implies a long
115 hiatus in the geological record, while $p\text{CO}_2$ built up from the low values necessary to
116 initiate low-latitude glaciation (0.1 or to 1 mbar) to those indicated by the
117 geochemical evidence. may have been characterized by cold, arid conditions
118 ~~represented only by t~~ The basal weathering horizon may record cold arid conditions
119 during part of this interval.

120 The evidence for ice-sheet advance/retreat cycles at low latitudes in a CO₂-
121 enriched atmosphere motivated a series of numerical simulations to test the
122 hypothesis that these cycles were linked to Milankovitch orbital variations. We
123 employed asynchronous coupling of a 3D ice sheet model and an Atmospheric
124 General Circulation Model using the continental configuration of (22). We first ran
125 simulations with a modern orbital configuration to examine ice-sheet behaviour
126 through a large range of $p\text{CO}_2$ values from 0.1 to 100 mbar, as used in previous
127 studies (23; Supplementary Figures 7-10). Consistently with previous results (2, 20),
128 at low $p\text{CO}_2$ (0.1 mbar), global ice volume reaches $170 \times 10^6 \text{ km}^3$ but substantial
129 tropical land areas remain ice free due to sublimation exceeding snowfall
130 (Supplementary Figure S10a). Ice volume remains relatively constant for $p\text{CO}_2 = 0.1$
131 to 20 mbar (Supplementary Figure S10b), due to an increase in accumulation that
132 compensates for higher ablation rates (Supplementary Figure 13). In contrast, above
133 20 mbar, ice extent in the eastern Tropics significantly decreases (Supplementary
134 Figure 10c). At $p\text{CO}_2 = 100$ mbar, most of the continental ice cover disappears except
135 for remnants over mountain ranges (Supplementary Figure 10d).

136 To test the sensitivity of the tropical ice sheets to Milankovitch forcing,
137 experiments with changing orbital parameters were initialized using the steady-state
138 ice sheets for $p\text{CO}_2 = 20$ mbar. Although obliquity has been invoked as a possible
139 cause of Neoproterozoic glaciations (24), this mechanism remains problematical and
140 cannot account for significant climatic oscillations at low latitudes (25, 26). We
141 therefore focused on precession as a possible driver, and used two opposite orbital
142 configurations favoring cold and warm summers, respectively, over the northern
143 tropics (CSO: cold summer orbit and WSO: warm summer orbit) (Supplementary

144 Figure 14). Switching between these configurations causes tropical ice-sheets to
145 advance/retreat over several hundred kilometers in 10 kyr (Supplementary Movie 1),
146 with strong asymmetry between hemispheres (Fig. 3). Shifting from WSO to CSO
147 causes ice retreat in the southern hemisphere, while ice sheet expansion occurs in
148 the northern hemisphere (Supplementary Figure 14c-d). Significant ice volume
149 changes occur between 30° N and S, but are less apparent in higher latitudes. This
150 reflects higher ablation rates in the warmer low latitudes (Supplementary Figure
151 14e-h), and higher ice-sheet sensitivity to shifting patterns of melt. Larger
152 greenhouse forcing at the end of the Snowball event implies increasing ice-sheet
153 sensitivity to subtle insolation changes. Given a strong diurnal cycle (23), our
154 simulations also predict a significant number of days above 0°C in the tropics
155 (Supplementary Figure 15), consistent with geological evidence for ice rafting, liquid
156 water in lakes and rivers, and photosynthetic microbial communities.

157 Our results show that geological evidence for glacial-interglacial cycles (5-7) is
158 consistent with an enriched Snowball Earth theory. Termination of the Marinoan
159 panglaciation was not a simple switch from icehouse to greenhouse states but was
160 characterized by a climate transition during which glacial cycles could be forced by
161 Milankovitch orbital variations. The geochemical evidence presented here implies
162 that at least the upper 60-70% of the Wilsonbreen Formation was deposited in $\sim 10^5$
163 years, on the assumption that a trend in $p\text{CO}_2$ would be evident over longer
164 timescales (21). Rates of CO_2 build-up, however, may have significantly slowed in the
165 later stages of Snowball Earth due to silicate weathering of exposed land surfaces, so
166 it is possible that the oscillatory phase was more prolonged.

Formatted: Font: Italic

Formatted: Subscript

167 ~~The Initiation of low latitude glaciation in the Neoproterozoic requires low $p\text{CO}_2$~~
168 ~~(0.1 - 1 mbar, 2, 19, 20), implying that the~~ oscillatory phase was preceded by a
169 prolonged period ($\sim 10^6$ to 10^7 years) during which $p\text{CO}_2$ gradually increased by
170 volcanic outgassing ~~(21) from the low levels (0.1 - 1 mbar) required for glacial~~
171 ~~initiation. In the Wilsonbreen Formation, this period appears to be represented~~
172 ~~solely by the basal weathering horizon, consistent with a 'deep Snowball' state with~~
173 ~~low temperatures and a limited hydrological cycle.~~ This timescale is consistent with
174 recent dating evidence for the duration of Cryogenian glaciations (27).

175 Additional work is needed to refine the upper and lower limits of $p\text{CO}_2$ conducive
176 to climate and ice-sheet oscillations in Snowball Earth. Factors not included in the
177 present model, such as supraglacial dust or areas of ice-free tropical ocean (28-30),
178 can be expected to make the Earth system more sensitive to orbital forcing. While
179 many details remain to be investigated, our overall conclusions remain robust.

180 The Neoproterozoic Snowball Earth was nuanced, varied and rich. We anticipate
181 that detailed studies of the rock record in other parts of the world, in conjunction
182 with numerical modeling studies, will continue to yield insight into the temporal and
183 regional diversity of this pivotal period in Earth history.

184

185

186 **Methods**

187

188 **Sedimentology.** Lithofacies were classified based on grain size, internal sedimentary
189 structures and deformation structures, and bounding surfaces. Detailed stratigraphic
190 logs were made in the field, supplemented by drawings and photographs of key

191 features. Samples were taken for polishing and thin sectioning, to allow detailed
192 examination of microstructures in the laboratory. In addition, data were collected on
193 clast lithology, shape, surface features and fabric. Diamictites of the Wilsonbreen
194 Formation are commonly very friable, allowing included clasts to be removed intact
195 from the surrounding matrix, allowing measurement of both clast morphology and
196 orientation, using methods developed for unlithified sediments. Clast morphology
197 (shape, roundness and surface texture) was measured for samples of 50 clasts to
198 determine transport pathways. Clast fabric analysis was performed by measuring a-
199 axis orientations of samples of 50 clasts with a compass-clinometer, and data were
200 summarized using the eigenvalue or orientation tensor method. Orientated samples
201 for measurement of Anisotropy of Magnetic Susceptibility (AMS) were collected
202 using a combination of field-drilling and block sampling. AMS was measured using an
203 AGICO KLY-3 Kappabridge operating at 875 Hz with a 300 A/m applied field at the
204 University of Birmingham and an AGICO MFK-1A Kappabridge operating at 976 Hz
205 with a 200 A/m applied field at New Mexico Highlands University.

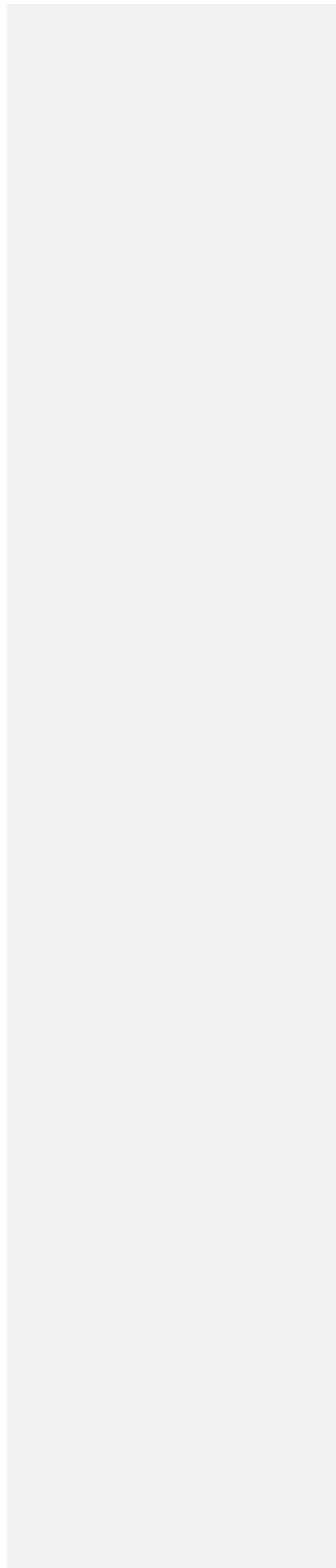
206

207 **Geochemistry.** Laboratory procedures for extracting, purifying, and measuring the
208 triple oxygen ($\delta^{18}\text{O}$ and $\Delta^{17}\text{O}$) and sulfur ($\delta^{34}\text{S}$) isotope composition of CAS in bulk
209 carbonates are detailed in ref 16. Briefly, fresh carbonate-bearing rock chips were
210 crushed into fine grains and powders using mortar and pestle. Rinsing the fines with
211 18 M Ω water revealed little water-leachable sulphate in all the Wilsonbreen
212 carbonates. Subsequently, ca. 10 to 30 g carbonates were slowly digested in 1-3 M
213 HCl solutions. The solution was then centrifuged, filtered through a 0.2 μm filter, and
214 acidified before saturated BaCl_2 droplets were added. BaSO_4 precipitates were

215 collected after >12 hours and purified using the DDARP method (see Supporting
216 Information). The purified BaSO₄ was then analyzed for three different isotope
217 parameters: 1) $\Delta^{17}\text{O}$, by converting to O₂ using a CO₂-laser fluorination method; 2)
218 $\delta^{18}\text{O}$, by converting to CO through a Thermal Conversion Elemental Analyzer (TCEA)
219 at 1450 °C; and 3) $\delta^{34}\text{S}$, by converting to SO₂ by combustion in tin capsules in the
220 presence of V₂O₅ through an Elementar Pyrocube elemental analyzer at 1050 °C. The
221 $\Delta^{17}\text{O}$ was run in dual-inlet mode while the $\delta^{18}\text{O}$ and $\delta^{34}\text{S}$ in continuous-flow mode.
222 Both the $\Delta^{17}\text{O}$ and $\delta^{18}\text{O}$ were run on a MAT 253 at Louisiana State University whilst
223 the $\delta^{34}\text{S}$ was determined on an Isoprime 100 continuous flow mass spectrometer at
224 the University of Lancaster, UK. The $\Delta^{17}\text{O}$ was calculated as $\Delta^{17}\text{O} \equiv \delta'^{17}\text{O} - 0.52 \times \delta'^{18}\text{O}$
225 in which $\delta' \equiv 1000 \ln (R_{\text{sample}}/R_{\text{standard}})$ and R is the molar ratio of ¹⁸O/¹⁶O or ¹⁷O/¹⁶O.
226 All δ values are in VSMOW and VCDT for sulphate oxygen and sulfur respectively.
227 The analytical standard deviation (1σ) for replicate analysis associated with the $\Delta^{17}\text{O}$,
228 $\delta^{18}\text{O}$, and $\delta^{34}\text{S}$ are $\pm 0.05\text{‰}$, $\pm 0.5\text{‰}$, and $\pm 0.2\text{‰}$, respectively. Since the CAS is
229 heterogeneous in hand-specimen, the standard deviation is for laboratory
230 procedures. $\delta^{34}\text{S}$ values were corrected against VCDT using within run analyses of
231 international standard NBS-127 (assuming $\delta^{34}\text{S}$ values of +21.1 ‰). Within-run
232 standard replication (1 SD) was <0.3 ‰. All geochemical data are included in
233 Supplementary Table 1.

234

235 Details of the numerical modelling are provided in the Supplementary Information in
236 the online version of the paper. Code for the GCM LMDz is freely available at:
237 <http://lmdz.lmd.jussieu.fr> but the ISM GRISLI (GRenoble Ice Shelf and Land Ice
238 model) is in limited access.



References

- (1) Hoffman, P.F. and Schrag, D.P. The Snowball Earth hypothesis: testing the limits of global change. *Terra Nova* **14**, 129-155 (2002).
- (2) Donnadieu, Y., Godd ris, Y. and Le Hir, G. Neoproterozoic atmospheres and glaciation. In: *Treatise on Geochemistry*, Second Edition Vol. 6, 217-229 (2014).
- (3) Hoffman, P.F. Strange bedfellows: glacial diamictite and cap carbonate from the Marinoan (635Ma) glaciation in Namibia. *Sedimentology* **58**, 57-119 (2011).
- (4) Allen, P.A. and Etienne, J.L. Sedimentary challenge to Snowball Earth. *Nat Geosci* **1**, 817-825 (2008).
- (5) Rieu, R., Allen, P.A., Pl tze, M. and Pettke, T. Climatic cycles during a Neoproterozoic 'snowball' glacial epoch. *Geology* **35**, 299-302 (2007).
- (6) Le Heron, D.P., Busfield, M.E., and Kamona, F. An interglacial on snowball Earth? Dynamic ice behaviour revealed in the Chuos Formation, Namibia. *Sedimentology* **60**, 411-427 (2013).
- (7) Fairchild, I.J. and Hambrey, M.J. Vendian basin evolution in East Greenland and NE Svalbard. *Precambrian Res* **73**, 217-233 (1995).
- (8) Halverson, G.P. A Neoproterozoic Chronology IN: Xiao, S. & Kaufman, A.J. (Eds.) *Neoproterozoic Geobiology and Paleobiology*, 231-271 (Springer, New York, 2006).
- (9) Li, X.-X., Evans, D.A. and Halverson, G.P. Neoproterozoic glaciations in a revised global palaeogeography from the breakup of Rodinia to the assembly of Gondwanaland. *Sediment Geol* **294**, 219-232 (2013).

(10) Petronis, M S, Stevenson, C, Fleming, E J, Fairchild, I J, Hambrey, M, Benn, D I., 2013, Paleomagnetic Data from the Neoproterozoic Wilsonbreen Formation, Ny Friesland, Svalbard, Norway and Preliminary Data from the Storeelv Formation, Ella Ø, Kong Oscar Fjord, East Greenland, American Geophysical Union, Fall Meeting 2013, abstract #GP41A-1107.

(11) Harland, W.B. *The Geology of Svalbard*. Geol. Soc. London Mem., 17 (Geological Society, London, 1997).

(12) Creveling, J.R. and Mitrovica, J.X. The sea-level fingerprint of a Snowball Earth deglaciation. *Earth Planet Sc Lett* **399**, 74–85 (2014).

(13) Lyons, W.B. et al. The McMurdo Dry Valleys long-term ecological research program: new understanding of the biogeochemistry of the Dry Valley lakes: a review. *Polar Geography* **25**, 202-217 (2001).

(14) Hoffman, P. et al. Are basal Ediacaran (635 Ma) basal 'cap dolostones' diachronous? *Earth Planet Sc Lett* **258**, 114-131 (2007).

(15) Fairchild, I.J., Hambrey, M.J., Spiro, B. and Jefferson, T.H. Late Proterozoic glacial carbonates in northeast Spitsbergen: new insights into the carbonate-tillite association. *Geol Mag* **126**, 469-490 (1989).

(16) Bao, H., Fairchild, I.J, Wynn, P.M. and Spötl, C. Stretching the envelope of past surface environments: Neoproterozoic glacial lakes from Svalbard. *Science* **323**,119-122 (2009).

(17) Cao, X. and Bao, H. Dynamic model constraints on oxygen-17 depletion in atmospheric O₂ after a Snowball Earth. *P Natl Acad Sci USA* **110**, 14546–14550 (2013).

(18) Le Hir, G. et al. The snowball Earth aftermath: Exploring the limits of continental weathering processes. *Earth Planet Sc Lett* **277**, 453–463 (2009).

(19) Pierrehumbert, R., Abbot, D.S., Voigt, A. and Koll, D. Climate of the Neoproterozoic. *Ann Rev Earth Planet Sci* **39**, 417-460 (2011).

(20) Pollard, D. and Kasting, J.F. Climate-ice simulations of Neoproterozoic glaciation before and after collapse to Snowball Earth. In: G.S. Jenkins, M.A.S. McMenamin, C.P. McKay and L. Sohl (eds.) *The Extreme Proterozoic: Geology, Geochemistry, and Climate*. Geophys. Monogr. Ser. 146 (AGU, Washington, D.C. 2004).

(21) Le Hir, G., Ramstein, G., Donnadiieu, Y. and Godd eris, Y. Scenario for the evolution of atmospheric pCO₂ during a snowball Earth. *Geology* **36**, 47–50 (2008).

(22) Hoffman, P.F., Li, Z.X., A palaeogeographic context for Neoproterozoic glaciation. *Palaeogeogr Palaeocl* **277**, 158–172 (2009).

(23) Pierrehumbert, R.T. Climate dynamics of a hard Snowball Earth. *J Geophys Res* **110**, DOI: 10.1029/2004JD005162 (2005).

(24) Spiegl, T. C., Paeth, H. and Frimmel, H.E., Evaluating key parameters for the initiation of a Neoproterozoic Snowball Earth with a single Earth System Model of intermediate complexity. *Earth Planet Sc Lett* **415**, 100-110 (2015).

(25) Donnadiieu, Y., Ramstein, G., Fluteau, F., Besse, J. and Meert, J. Is high obliquity a plausible cause for Neoproterozoic glaciations? *Geophys Res Lett* **29**, DOI: 10.1029/2002GL015902 (2002).

(26) Paillard, D. Quaternary glaciations: from observations to theories. *Quaternary Sci Rev* **107**, 11-24 (2015).

(27) Rooney, A.D. et al. ~~Re-Os geochronology and coupled Os-Sr isotope constraints on the Sturtian snowball Earth. PNAS 111, doi: 10.1073/pnas.1317266110A~~ Cryogenican chronology: Two long-lasting synchronous Neoproterozoic glaciations. *Geology* 43, 459-462 (20152014).

(28) Abbot, D.S. and Pierrehumbert, R.T. Mudball: surface dust and Snowball Earth deglaciation. *J Geophys Res* **115**, DOI: 10.1029/2009JD012007 (2010).

(29) Abbot, D.S., Voigt, S. and Koll, D. The Jormungand global climate state and implications for Neoproterozoic glaciations. *J Geophys Res-Atmos* 116, DOI: 10.1029/2011JD015927 (2011).

(30) Rose, B. E. J. Stable “Waterbelt” climates controlled by tropical ocean heat transport: A nonlinear coupled climate mechanism of relevance to Snowball Earth. *J Geophys Res-Atmos* **120**, doi:10.1002/2014JD022659 (2015).

Correspondence and requests for materials should be addressed to Doug Benn (doug.benn@unis.no).

Acknowledgements

This work was supported by the NERC-funded project GR3/ NE/H004963/1 Glacial Activity in Neoproterozoic Svalbard (GAINS). Logistical support was provided by the University Centre in Svalbard. This work was granted access to the HPC resources of CCRT under allocation 2014-017013 made by GENCI (Grand Equipement National de Calcul Intensif). We also thank Didier Paillard and Paul Hoffman for stimulating discussions and valuable insights.

Author contributions

Field data were collected and analyzed by IJF, DIB, EJF, MJH, EAMcM, MSP, PMW and CTES. Geochemical analyses were conducted by HB and PMW. Model experiments were designed and conducted by GLeH, YD, CD and GR. The manuscript and figures were drafted by DIB, IJF and GLeH, with contributions from the other authors.

Competing financial interests

The authors declare no competing financial interests.

Figures:

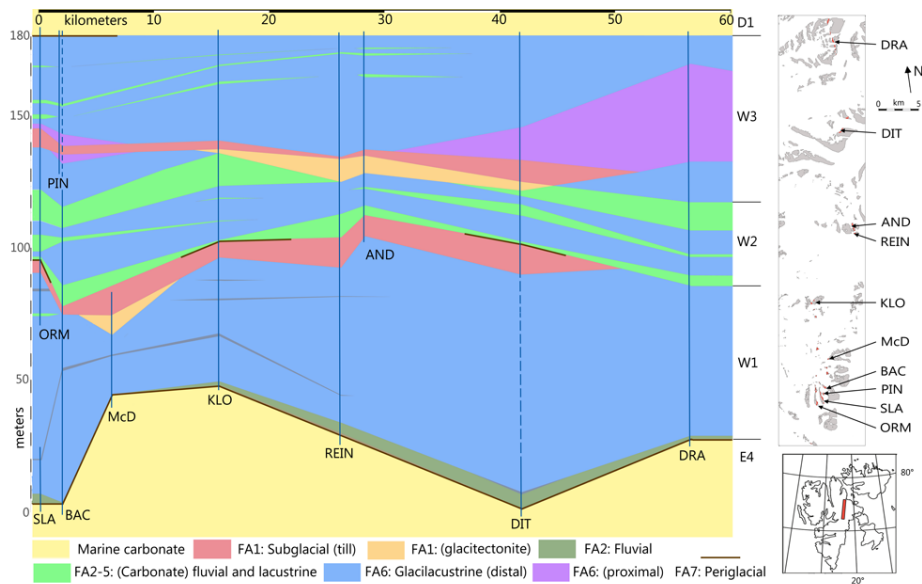


Figure 1: Sedimentary architecture and palaeoenvironments of the Wilsonbreen Formation. Regional correlation of facies associations and members W1, W2 and W3 across NE Svalbard. From north to south, study locations are: DRA: Dracoisen; DIT: Ditlovtoppen; AND: East Andromedafjellet; REIN: Reinsryggen (informal name); KLO: Klofjellet; McD: MacDonaldryggen; BAC: Backlundtoppen - Kvitfjellet ridge; PIN: Pinnsvinryggen (informal name); SLA: Slangen and ORM: Ormen.

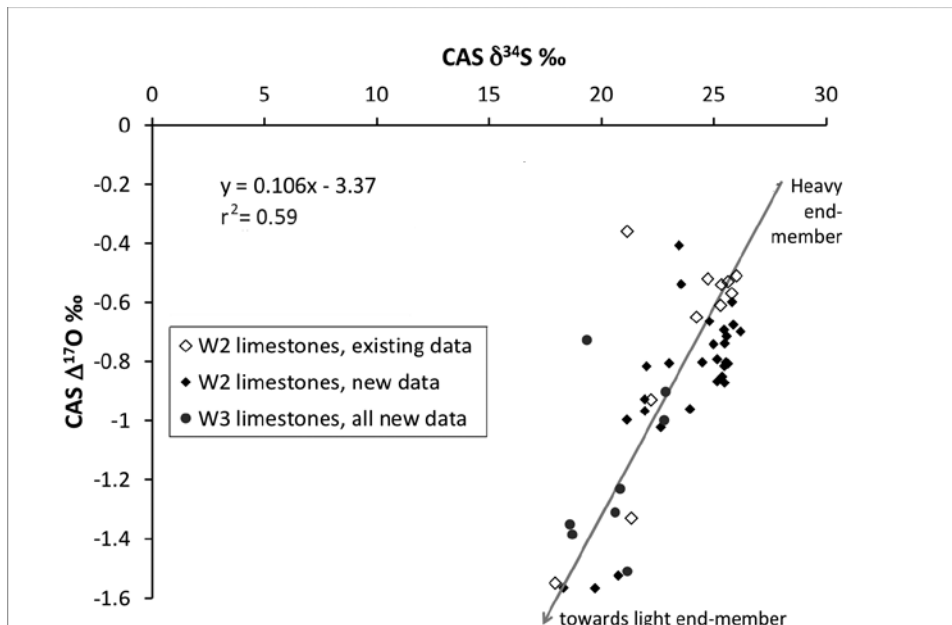


Figure 2: Co-variation of $\Delta^{17}\text{O}$ and $\delta^{34}\text{S}$ from carbonate-associated sulphate in W2 and W3. 'Existing data' (ref. 16) and new data define a mixing line between pre-glacial sulphate (top) and an isotopically light sulphate formed by oxidation of pyrite including incorporation of a light- $\Delta^{17}\text{O}$ signature from a CO_2 -enriched atmosphere. Data from W2 and W3 lie on closely similar trend lines, indicating no detectable change in $p\text{CO}_2$ between deposition of the two members.

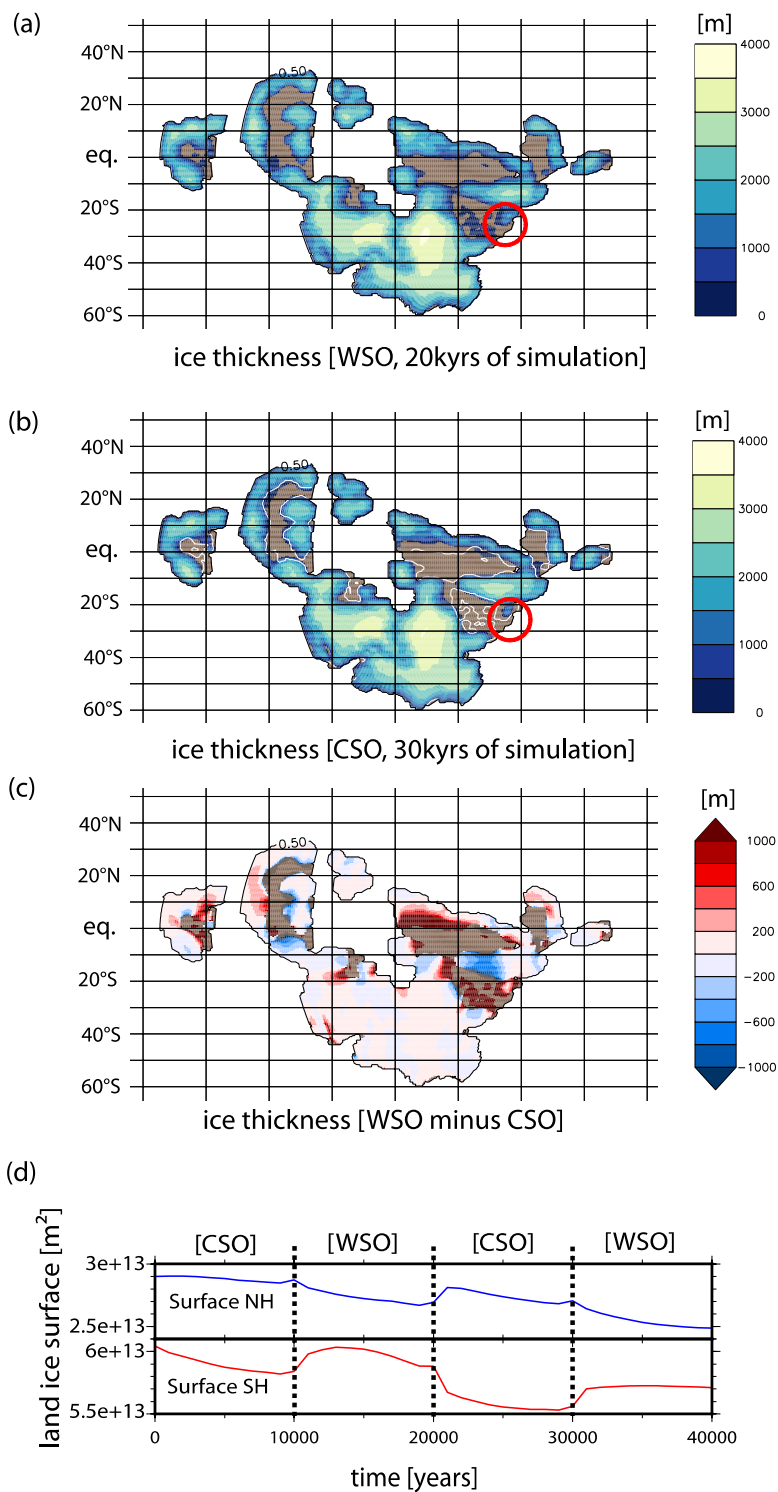


Figure 3: Modelled ice sheet oscillations in response to orbital forcing. (a), (b)

shaded contours show land ice thickness obtained with 20 mbar of carbon dioxide in response to changes of orbital forcing (WSO and CSO, warm/cold summer orbit for the northern hemisphere) over the course of two precession cycles (40 ky of simulation). In light brown continental areas without ice, the white line is used to represent the old ice-sheet extension (WSO case). The Svalbard area is indicated by a red circle. (c) ice thickness variation in 10 ky (WSO case after 20 ky minus CSO case after 30 ky of simulation) (d) surface of hemisphere covered by ice (m^2) through time ([WSO] and [CSO] indicate which orbital configuration is used).